RESEARCH ARTICLE   OPEN ACCESS

An Improved Direct Torque Control for Three-Level Inverter-Fed Induction Motor Drive

Papi Naidu Tentu[1,] Prof K.Vijay Kumar [2]

[1] Pg Student, Dadi Institute Of Engg.& Tech, Anakapalle, Visakhapatnam,Andhra Pradesh, India.
[2] professor, Dept.Of Eee, Dadi Institute Of Engg.& Tech, Visakhapatnam,.India.

ABSTRACT
A three-level neutral-point-clamped inverter-fed induction motor drive is proposed in this paper. The conventional direct torque control (DTC) switching table fails to consider the circuit limitations, such as neutral-point-balance and smooth vector switching, caused by the topology of a three-level inverter. Two kinds of modified schemes for three-level DTC are proposed to solve these problems. They provide performance enhancement while maintaining robustness and simplicity.
In the present project the DTC is performed by using space vector pulse width modulation (SVPWM) technique in order to achieve smooth operation of drive.
Fuzzy logic control and the speed-adaptive flux observer are introduced to enhance the performance of the system. The issue of large starting current can be investigated and solved by introducing the technique of pre-excitation. The effectiveness of the proposed schemes is confirmed by simulation using MATLAB/SIMULINK implementation and experimental validation.

Index Terms — AC motor drives, adaptive observer, fuzzy logic, induction motor (IM) drives, three-level inverter, torque control.

I.   INTRODUCTION

Direct torque control (DTC) has emerged as an alternative to field-oriented control (FOC) for high-performance ac drives, since it was first proposed in the mid-1980s .The merits of DTC can be summarized as fast torque response, simple structure (no need of complicated coordinate transformation, current regulation, or modulation block), and robustness against motor parameter variation. On the other hand, multilevel inverters have attracted considerable attention, especially in high-power application areas. The three-level neutral-point-clamped (NPC) inverter is one of the most commonly used multilevel inverter topologies in high-power ac drives.

Compared to the standard two-level inverter, the three-level inverter presents its superiority in terms of lower voltage distortion, lower stress across the semiconductors, less harmonic content, and lower switching frequency. Because of these merits mentioned, the three-level inverter-fed DTC motor drive has become an important research topic in industry and the academic community over the past decades.

Compared to two-level DTC, three-level DTC motor drives have two particular aspects. The first is concerned with electromagnetic performance enhancement, including torque ripple reduction and low-speed performance improvement in a similar manner to that of two-level DTC.

The second is inherited from the topology of three-level inverter, i.e., the neutral point potential balance and smooth vector switching. Neutral point unbalance will cause higher voltage in the power semiconductors. This increases the demand of capacity so that the cost increases. The balance of neutral point potential can be achieved by exploiting the opposite effect of redundant vectors on the neutral point potential.

Smooth vector switching requires that there is no excessive voltage "jumps" in both phase voltage and line voltage. Phase voltage "jumps" fail to utilize the advantages of three-level inverter and may endanger the safe operation of inverter by causing full dc voltage across one switch during transient commutation, especially when the inverter uses only one snubber circuit for three phases. Line voltage "jumps" produce more harmonic content in output voltage waveform, which is unfriendly to the motor and increase the burden on the filter.

Most of the literature on three-level inverter DTC motor drives concentrates on performance improvement. These employ complicated algorithms based on analytical methods, coordinate transformation, and continuous space vector modulation, among others.

Although good performance, such as torque ripple reduction or fixed switching frequency, was achieved, they failed to consider the limitations caused by the circuit topology, i.e., neutral point potential balance and smooth vector switching was almost not mentioned at all.

However, there still exists the possibility of undesired excessive line voltage jumps, e.g., from ++− to + - - . The aim of this paper is to achieve high-

performance DTC for a three-level inverter-fed induction motor (IM) drive, as well as considering the neutral point potential balance and smooth vector switching.
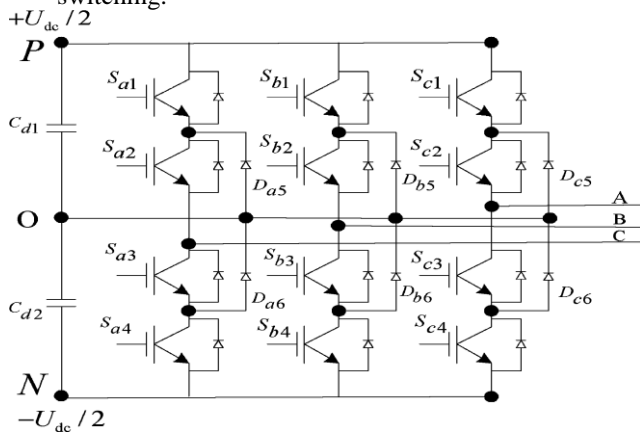

Fig 1.1 BASIC THREE LEVEL INVERETR

Two kinds of DTC schemes are proposed to obtain high-performance control of torque and stator flux and the switching principle is illustrated to meet the limitations required by the topology of three-level inverter. As DTC is often referred for its drawbacks of large starting-up current and flux droop at low speed, the technology of pre-excitation is introduced to limit the starting current.

To enhance the low-speed performance, a fuzzy logic controller (FLC) is incorporated in the outer speed loop to improve the speed response and a speed-adaptive flux observer with novel gain and load torque observation is employed to estimate stator flux, torque, and rotor speed over a wide speed range.

Simulations, as well as experimental results, are presented to validate the effectiveness of the schemes proposed in this paper.

II. PRINCIPLE OF DTC AND THREE-LEVEL INVERTER

2.1. Three-Level Inverter

The main circuit of a three-level inverter is illustrated in Fig. 1.1 and there are three states for one-phase output: $+U$dc/2, 0, and $-U$dc/2, with the neutral point as reference. To be more universal, the negative dc bus voltage will be selected as reference ground, and the three states are indicated by "2," "1," and "0," for "$+U$dc/2," "0," and "$-U$dc/2," respectively. More output levels provide more freedom in vector selection and it is possible to synthesize waveforms that are more sinusoidal in shape. However, the complexity of vector selection rises with the number of vectors. In addition, there are further problems, including neutral point balance and smooth vector switching, which need to be carefully solved.

2.2. Basic Principle of DTC

A mathematical model of an IM described by space vectors in a stationary frame can be expressed as follows

$$u_s = R_s\, i_s + p\, \psi_s \qquad 2.1$$
$$0 = R_r\, i_r + p\, \psi_r - j\omega_r\, \psi_r \qquad 2.2$$
$$\psi_s = L_s\, i_s + L_m\, i_r \qquad 2.3$$
$$\psi_r = L_m i_s + L_r\, i_r \qquad 2.4$$

where u_s, i_s, i_r, ψ_s, and ψ_r are the stator voltage vector, stator current vector, rotor current vector, stator flux linkage vector, and rotor flux linkage vector, respectively; R_s, R_r, L_s, L_r, and L_m are the stator resistance, rotor resistance, stator inductance, rotor inductance, and mutual inductance, respectively; and ω_r is the rotor speed and $p = d/dt$ is the differential operator.

From the stator voltage equation (2.1), it can be seen that, by omitting the stator resistance voltage drop, the stator flux can be controlled directly from the stator voltage. The electromagnetic torque can be obtained from

$$Te = \frac{3}{2}\, Np\, \frac{Lm}{\sigma\, Ls\, Lr}\, \psi r * \psi s = Te = \frac{3}{2}\, Np$$
$$\frac{Lm}{\sigma\, Ls\, Lr}\, \| \psi r \| \| \psi s \|\, Sin\delta sr \qquad 2.5$$

where δ_{sr} is the spatial angle between the stator and rotor fluxes, N_p is the motor pole-pair number, and T_e is the electromagnetic torque. In DTC, the amplitude of the stator flux is kept constant and a fast torque response is obtained by changing angle δ_{sr} quickly. From (2.1)–(2.4), the relationship between the stator and rotor fluxes can be obtained as

$$P\, \psi r + (\frac{1}{\sigma\, Tr} - jWr)\, \psi r = \frac{Lm}{\sigma\, Ls\, Tr}\, \psi s \qquad 2.6$$

where $\sigma = 1 - L_2\, m/(L_s L_r)$ and $T_r = L_r/R_r$. Equation (2.6) indicates that the dynamic response of the rotor flux is a first-order lag with respect to the stator flux, so the torque can be changed quickly by changing the angle of stator flux.

III. TORQUE AND FLUX RIPPLE REDUCTION IN DTC

The conventional switching table for two-level DTC cannot be directly extended to three-level DTC. This is because it is not only the performance that is of concern, the limitation caused by the topology of three-level inverter also should be considered. Two kinds of scheme for three-level DTC are proposed in this paper to solve these problems.

3.1. DTC Method - I

The first DTC scheme utilizes the vectors of the three-level inverter directly and inserts appropriate intermediate vectors to meet the demand of neutral point balance and smoothed vector switching.The switching principle is described in detail in the following. First, the vector is selected according to the demand of the flux and torque; vector switching and neutral point balance will be considered later. Fig.3.1 shows the space vector diagram for a three-level DTC

control strategy and its sector division. The 27 vectors are marked by $V_1, V_2 \ldots V_{27}$. There are 12 sectors and the shadowed area is the first sector, which is different from that of the conventional two-level DTC. The basic principles of the vector selection are shown in Table 3.1 and these meet the demands of the flux and torque; k represents the stator flux located in k^{th} sector. In addition, "↑" means increase, "↓"means decrease, and "="means no change is needed.
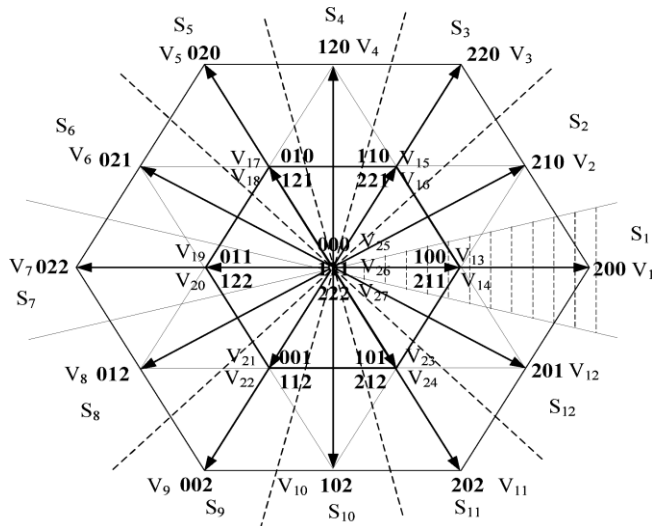

Fig. 3.1. SPACE VECTOR DIAGRAM FOR THE THREE-LEVEL DTC.

TABLE 3.1
VECTOR SELECTION TABLE FOR THREE-LEVEL DTC

Flux	Torque	Selected vector number
	↑	k+2
↑	=	26
	↓	k-2
	↑	k+4
↓	=	26
	↓	k-4
	↑	k+3
↑	=	26
	↓	k-3

It should be noted that there may exist more than two vectors to meet the demands of the flux, and the one which meets the torque response better is preferred. However, in many cases, the selected vector usually cannot meet the requirements of the vector switching and neutral point balance, which means that the selected vector cannot be applied to the three-level inverter directly.

For example, suppose the stator flux is located in the first sector, and the working voltage vector at the moment is $V_1(200)$. To increase the stator flux and torque, according to Table 3.1, $V_3(220)$ would be selected. But there is a high-voltage jump in phase B from 0 to 2, which should be avoided. In this case, $V_2(210)$ will be inserted as an intermediate vector to smooth the high-voltage jump.

There are three aspects with respect to voltage jumps: 1) phase voltage jump, 2) line voltage jump, and 3) three-phase jump at the same time.

High-voltage jump increases harmonic content and the stress across power semiconductors, which negates the advantages of the three-level inverter. To overcome this problem, an appropriate intermediate vector should be inserted to meet the requirement of the voltage jump.

Another issue is the problem of neutral point balance, which is inherited from the topology of three-level inverter. Neutral point balance is mainly controlled by selecting appropriate small vectors; this is because of the opposite effects of redundant vectors.

In this paper, we also adopt the redundant states of small vectors to keep the neutral point balance.

The final vector selection rules are obtained by considering the aspects introduced earlier, and the principles are summarized as follows.

Step I: Select vector according to the demands for flux and torque, which are listed in Table 3.1.
Step II: If the selected vector cannot meet the requirement of the voltage jump and neutral point
        balance, an appropriate intermediate vector will be inserted.

The principles for selecting the intermediate vectors are as follows.
1) Large vectors or middle vectors should be selected preferably to increase the utilization ratio of the dc bus.
2) Middle vectors can switch to adjacent small vectors and large vectors freely.
3) Large vectors can switch to the small vectors in the same spatial orientation.
4) Small vectors can switch to zero vectors freely.
5) When small vectors are available, select the one, which can meet the requirement of neutral Point balance. Using the steps earlier, an appropriate vector can be selected to meet the demand of the flux and torque, as well as the requirement of voltage jump and neutral point balance, which ensures the safe operation of the three-level inverter.

3.2. DTC Method - II
In DTC method -I, by inserting the appropriate intermediate vector, the problems of neutral point balance and smooth vector switching were solved. However, it may degrade the performance of torque and increase the complexity of vector selection, so another scheme is proposed here.

Method - II makes use of synthesizing vectors, which is termed discrete space vector modulation (SVPWM). This was first proposed in two-level DTC. The two-level SVPWM-DTC incorporates a more complicated and accurate switching table by dividing one sampling period into

two or three intervals, and thus, more vectors are obtained.

Speed is also taken into account and more levels of hysteresis are adopted to make the switching table more accurate. The benefits of SVPWM-DTC are reduced torque and flux ripple at a little extra expense of computational time.

This paper extends SVPWM to three-level DTC by using synthesizing vectors and the main aim of introducing SVPWM is to solve the problems of neutral point balance and smooth vector switching. To reduce the complexity of the algorithm, the same structure as Table 3.1 is adopted and the speed was not taken into account in the switching table. First, we should synthesize some vectors, which are expected to solve the problems of neutral point balance and smooth switching between any two vectors simultaneously.

This means that the vector selection, according to the need of the torque and flux, is decoupled from the circuit limitation introduced by the three-level topology. A series of novel synthesizing vectors are produced, which are illustrated in Fig. 3.2 and marked by V_{s1}, V_{s2}, . . . , V_{s12}.

Take V_{s1} , for example, it is synthesized by the nearest three vectors, namely, V_1(200), V_2 (210), and V_{13}/V_{14} (100/211). The duration time of each vector can be calculated easily by utilizing the principle of volt-second balance. To smooth the vector switching, zero vector V_{26}(111) is incorporated at the beginning and ending of each synthesize sequence, taking up 10% or less duty of the whole period.

The 12 synthesizing vectors are distributed uniformly in the fixed-angle space (15° for V_{s1}) with constant or variable amplitude.

In this paper, constant amplitude for the synthesis vector is selected for simplicity, so the duration of each vector in V_{s1} ,V_{s2} , . . . ,V_{s12} can be obtained offline and stored in a look-up table for real time implementation. The final synthesizing vectors are listed in Table 3.2 and the sector division for three-level DTC is presented in Fig. 3.2, which has a 15° shift compared to that in Fig. 3.1. From Table 3.1, it is seen that the switching between any arbitrary two vectors or adjacent vectors in a synthesis sequence are smooth. The neutral point balance can be solved by adjusting the "lasting time" of the small vectors in one sampling period. Taking V_{s1} as an example, 211 and 100 are a pair of small vectors and their total "lasting time" is fixed during one sampling period, but their individual working time can be arranged according to the requirement of neutral point balance.
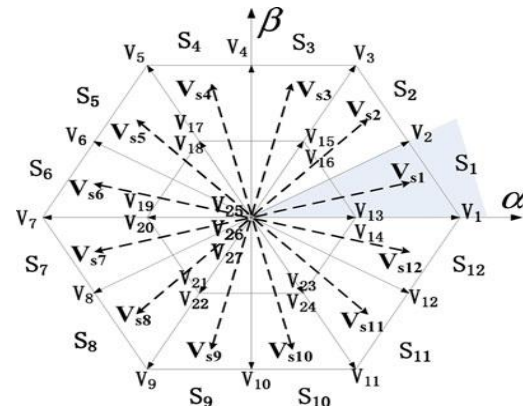

Fig. 3.2 SYNTHESIS VECTOR DIAGRAM.

TABLE 3.2
NOVEL VECTOR SYNTHESIS

Vector no.	Vector synthesis sequence
V_{s1}	111-211-210-200-100-200-210-211-111
V_{s2}	111-110-210-220-221-220-210-110-111
V_{s3}	111-110-120-220-221-220-120-110-111
V_{s4}	111-121-120-020-010-020-120-121-111
V_{s5}	111-121-021-020-010-020-021-121-111
V_{s6}	111-011-021-022-122-022-021-011-111
V_{s7}	111-011-012-022-122-022-012-011-111
V_{s8}	111-112-012-002-001-002-012-112-111
V_{s9}	111-112-102-002-001-002-102-112-111
V_{s10}	111-101-102-202-212-202-102-101-111
V_{s11}	111-101-201-202-212-202-201-101-111
V_{s12}	111-211-201-200-100-200-201-211-111

DTC method-II employs the same switching table, as shown in Table 3.1, except that the selected vector is replaced by the novel synthesis vector listed in Table3.2. For example, if the selected vector number is *k* according to Table 3.1, the synthesized vector V_{sk} will be selected as the output vector, and number 26 means the zero vector 111.

For DTC method - I, a further step- II should be taken before the final vector is selected; however, this process is not needed in method-II, which simplifies the selection of vector. An example of switching pattern for the two kinds of DTC method is illustrated in Fig. 3.3. It is seen that for DTC method-I, there is only one vector in one sampling period, while there is a sequence of vectors for DTC method - II, with 111 as the beginning and ending.
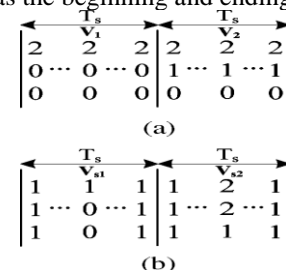

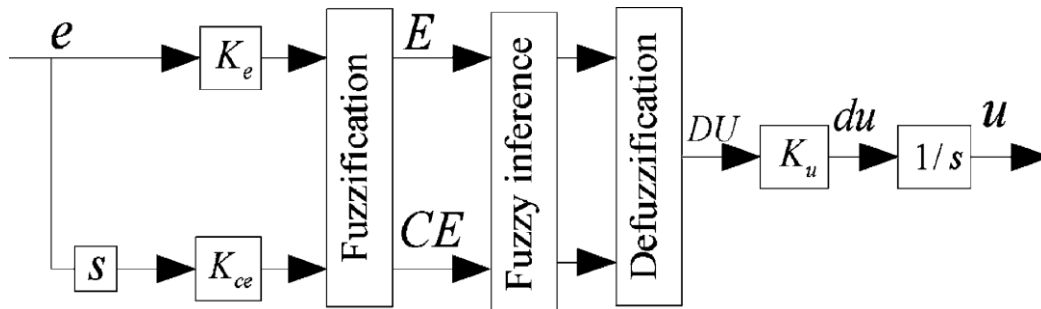Fig. 3.3 Example of switching pattern. (a) DTC method I. (b) DTC method II.

Fig. 3.4. Diagram of the FLC.

IV.   PERFORMANCE ENHANCEMENT OF DTC

To enhance the dynamic performance and steady-state accuracy, as well as robustness to external disturbance and motor parameters variations, FLC is used in the outer speed loop. Furthermore, a full-order speed-adaptive flux observer with novel gains is employed in this paper, and a load torque observation is introduced to improve the dynamic response of the speed estimation. Also, the well-known problem of large start-up current in DTC is addressed by introducing the technique of pre excitation. These three aspects are described in this section in detail.

4.1 Fuzzy Logic Speed Control

FLC can handle complicated nonlinear systems, which have a degree of uncertainty. It does not require exact system modeling and parameters; this makes FLC very suitable for motor drive control. A classical FLC is composed of three parts: fuzzification of input variables, fuzzy reasoning, and defuzzification. A diagram for the FLC used in this paper is illustrated in Fig. 4.1. The inputs are the error between commanding value and real value, and its derivative. The output is the control increment du, whose integral is the real output.
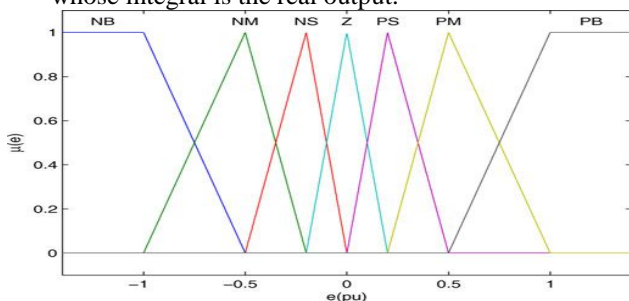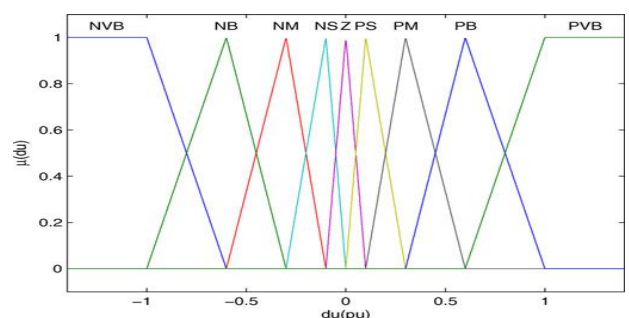

Fig. 4.1 Input membership function.

Fig.4.2. Output membership function.

The input and output variables are scaled to the range of (-1.4, 1.4). For the input variables, there are seven variables defined in the fuzzy sets: PB,PM, PS, Z, NS, NM, and NB in descending order. To improve the dynamic performance and obtain more refined output, two other variables are added in the fuzzy sets for the output variables, i.e., PVB and NVB. Figs. 6 and 7 show the membership functions of the inputs and the output, respectively. To obtain a fast response for dynamic performance, and high accuracy for steady state, the asymmetric triangle is selected as the membership function, which is different from the conventional design. Table III shows the inference rule used in this paper, which is the key part of the FLC. By careful design of the inference rule, excellent performance can be achieved. The mapping relationship between the input and the output variable is illustrated in Fig. 4.3.

4.2 Speed-Adaptive Flux Observer

Motor drives can work in a hostile environment, which increases their reliability and decreases their complexity and the cost of the system. Hence, operation is very attractive proposition in many industrial applications. Among various approaches, observer-based techniques are very popular and versatile. Compared with open-loop speed estimation techniques, the observer-based methods are more robust to motor parameter variations because they introduce an error feedback of the stator current estimation. In a classical observer, the gain is such designed that the poles of observer are proportional to those of the IM (usually a factor $k > 1$). This strategy of gain selection results in poles with large imaginary parts, which may cause instability in high-speed operation. In addition, the observer gain usually contains speed-dependent terms, which may be affected by the accuracy of the observed speed. This paper adopts a speed-adaptive flux observer with novel gains to improve the stability of the system. Load torque observation is also incorporated to enhance the dynamic response of the speed estimation. The mathematical model of the observer can be expressed as follows

$$P\,i_s = -[(\frac{1}{\sigma Ts} + \frac{1}{\sigma Tr}) - jWr]\,i_s +$$

$$\frac{1}{\sigma Ls}(\frac{1}{Tr} - jWr)\,\psi s +$$

$$\frac{1}{\sigma\,Ls}\,us + G1(is - i\hat{}_s) \qquad -$$
4.1

$$P\,\psi\hat{s} = -Rsis$$

$$+us+ G2(is - i\hat{}_s) \qquad - 4.2$$

$$P\,\hat{W}r = \frac{p}{j}(\hat{T}_e - \hat{T}_L) + K_w\,[\Delta i_s *$$

$$(\lambda L_r\,\hat{\psi}s - i\hat{}_s)] \qquad -$$
4.3

$$P\,\hat{T}_L = - K_T\,[\Delta i_{s*}(\lambda L_r\,\hat{\psi}s - i\hat{}_s)] \qquad -$$
4.4

TABLE 4.1
RULE MATRIX OF FLC

Output		E						
		NB	NM	NS	Z	PS	PM	PB
	NB	NVB	NVB	NVB	NB	NM	NS	Z
	NM	NVB	NVB	NB	NM	NS	Z	PS
	NS	NVB	NB	NM	NS	Z	PS	PM
CE	Z	NB	NM	NS	Z	PS	PM	PB
	PS	NM	NS	Z	PS	PM	PB	PVB
	PM	NS	Z	PS	PM	PB	PVB	PVB
	PB	Z	PS	PM	PB	PVB	PVB	PVB
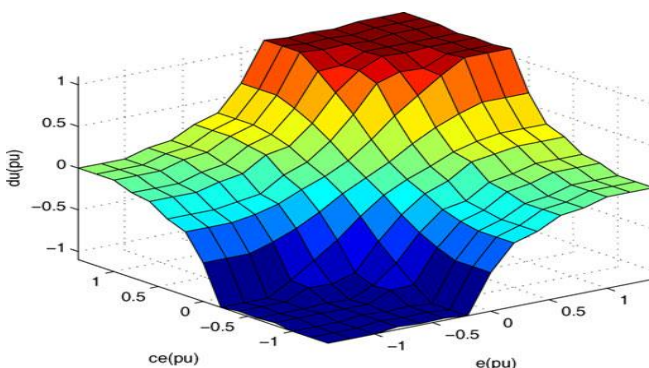
Fig. 4.3 . Control surface of FLC.

$g_{1r} = 2b$		4.5
$g_{1i} = 0$		4.6
$g_{2r} = \sigma\,L_s b$		4.7
$g_{2i} = 0$		4.8

Where *b* is a negative constant gain

4.3 Decreasing Starting Current

To decrease the starting current and maintain sufficient starting torque, pre excitation of the stator flux is proposed in this paper. For an open-loop *V / f* motor drive, the starting current is restricted by switching between nonzero and zero vectors according to the error between the reference and measured currents. It cannot control the stator flux accurately because no observer or estimator is employed to obtain the stator flux as a feedback.

In the system proposed here, as an adaptive flux observer is incorporated in the system, the stator flux can be controlled accurately and achieve the pre excitation in the true sense. It should be noted that current limitation is needed and it works only during the pre excitation process, because the magnetization process without current limitation still produces undesired large current. However, the current limit in the pre excitation does not have to be large to produce the needed stator flux.

The amplitude of current limitation only affects the lasting time of pre excitation. In this paper, the current limit it set to be 80% of rated current. During the pre excitation process, when the current exceeds the imitation setting, a zero vector will be selected to reduce the current; otherwise a fixed vector will be selected to produce stator flux, which acts in a bang-bang fashion. When stator flux tilts the lower limit of flux hysteresis, the process of pre excitation is terminated and the motor can start with sufficient torque by DTC, because there is sufficient flux to produce torque. In all, the three-level DTC drive can restrict the start-up current effectively and establish accurate stator flux at the same time, which benefits from the flux observation employed in the system.

V. SIMULATION AND EXPERIMENTAL RESULTS

To validate the effectiveness of the two DTC methods, a three-level DTC motor drive is developed and experimental results are presented here. The three-level DTC drive is illustrated in Fig.5.1. FLC is employed in the outer speed loop for speed control, and a speed-adaptive flux observer with load torque observation is used to estimate the rotor speed, stator flux, and torque. The estimated states are fed back to the outer loop of speed, flux, and torque. The motor inertia is 0.05 kg / m^2, and the sampling frequency of system for DTC method I and II are 30 and 10 kHz, respectively
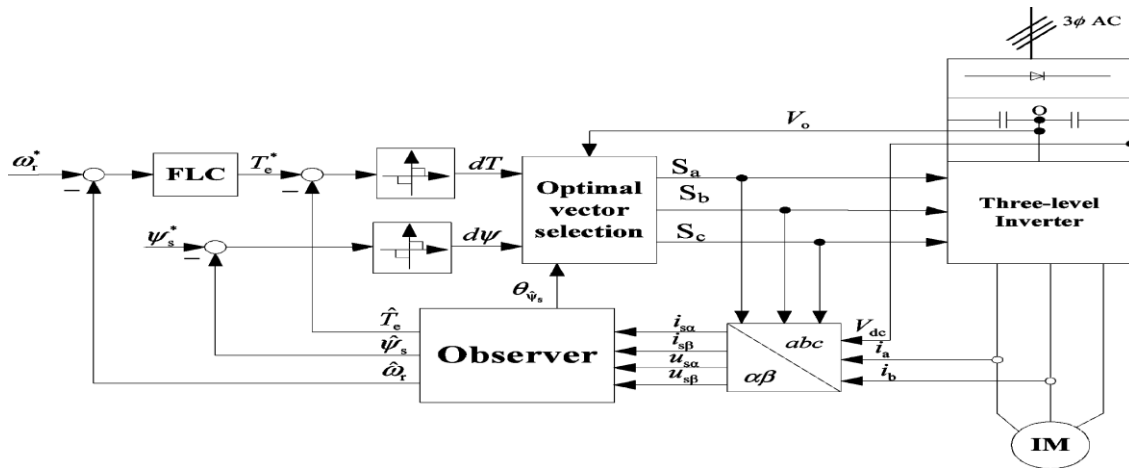
Fig. 5.1 Three-level DTC drive.
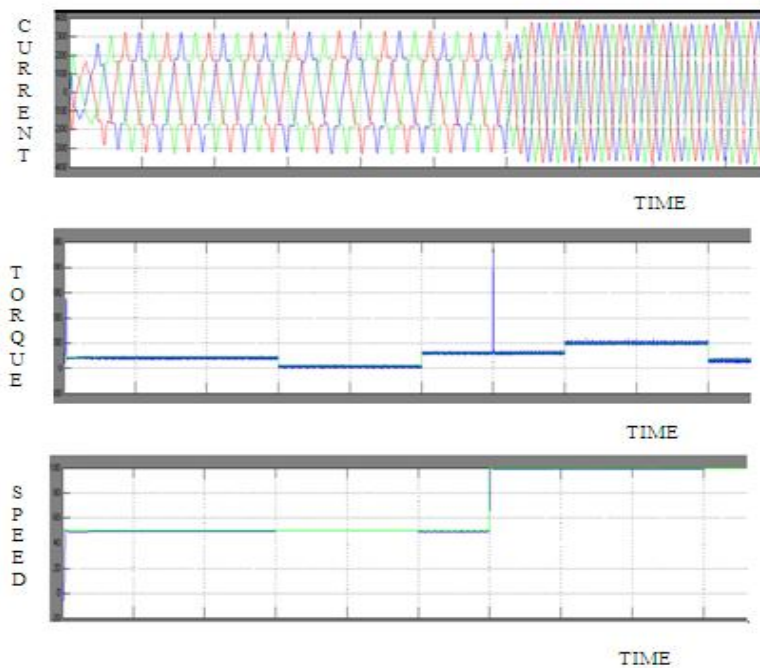
SIMULATION AND EXPERIMENT PARAMETERS

Fig 5.1 Starting response of DTC method I with pre excitation.

Figs. 5.1 show the starting response for DTC method I from 0 to 1200 r/min, and with and without pre excitation, respectively. In Fig. 5.1 , the stator flux is first established by using the pre excitation technique, which can be seen from the upper half in Fig. 5.1. The motor then accelerates up to 1200 r/min with the permitted maximum torque. The maximum starting current is restricted to 7.5 A; this value reaches almost 27 A without pre excitation. The stator flux is established with current limitation before starting the motor, so sufficient torque can be produced, which may result better dynamic performance. However, the dynamic response difference between the one with and without pre excitation is not significant, if the pre excitation time is excluded; this is because the stator flux can be established in several milliseconds, unfortunately, at the expense of large current.

VI. CONCLUSION

Two kinds of modified DTC schemes have been proposed in this paper and both achieve high-performance control of a three-level inverter-fed motor drive. They both work over a wide speed range and overcome the limitations caused by the topology of the three-level inverter. By using appropriate intermediate vectors, the problems of neutral point balance and smooth vector switching are solved. Furthermore, a novel vector synthesis sequence was proposed and this decoupled the performance control from the circuit limitation. A FLC and a speed-adaptive flux observer were incorporated in the drive

to enhance the performance of system. In addition, the issue of large starting current are investigated and solved by introducing the technique of pre excitation. Very low speed operation of 6 r/min was demonstrated. Simulations as well as experimental results were presented to verify the effectiveness of the proposed schemes.

REFERENCES

[1] I. Takahashi and T. Noguchi, "A new quick-response and high-efficiency control strategy of an induction motor," *IEEE Trans. Ind. Appl.*, vol. IA-22, no. 5, pp. 820–827, Sep. 1986.

[2] M. Depenbrock, "Direct self-control (DSC) of inverter-fed induction machine," *IEEE Trans. Power Electron.*, vol. 3, no. 4, pp. 420–429, Oct. 1988.

[3] Y. Zhang and J. Zhu, "Direct torque control of permanent magnet synchronous motor with reduced torque ripple and commutation frequency," *IEEE Trans. Power Electron.*, vol. 26, no. 1, pp. 235–248, 2011.

[4] D. Casadei, G. Serra, and A. Tani, "Improvement of direct torque control performance by using a discrete svm technique," in *Proc. PESC 1998 Record Power Electron. Spec. Conf. 29th Annu. IEEE*, May 17–22, vol. 2, pp. 997–1003.

[5] G. S. Buja and M. P. Kazmierkowski, "Direct torque control of PWM inverter-fed AC motors—A survey," *IEEE Trans. Ind. Electron.*, vol. 51,no. 4, pp. 744–757, Aug. 2004.

[6] J. Rodriguez, S. Bernet, B.Wu, J. Pontt, and S.Kouro, "Multilevel voltagesource-converter topologies for industrial medium-voltage drives," *IEEE Trans. Ind. Electron.*, vol. 54, no. 6, pp. 2930–2945, Dec. 2007.

[7] W. Yao, H. Hu, and Z. Lu, "Comparisons of space-vector modulation and carrier-based modulation of multilevel inverter," *IEEE Trans. Power Electron.*, vol. 23, no. 1, pp. 45–51, Jan. 2008.

[8] S. Busquets-Monge, S. Alepuz, J. Bordonau, and J. Peracaula, "Voltage balancing control of diode-clamped multilevel converters with passive front-ends," *IEEE Trans. Power Electron.*, vol. 23, no. 4, pp. 1751–1758, Jul. 2008.

[9] Y. Zhang and Z. Zhao, "Study on capacitor voltage balance for multi-level inverter based on a fast SVM algorithm," *Proc. CSEE*, vol. 26, no. 18, pp. 71–76, 2006, (in Chinese).

[10] L. Dalessandro, S. D. Round, and J. W. Kolar, "Center-point voltage balancing of hysteresis current controlled three-level pwm rectifiers," *IEEE Trans. Power Electron.*, vol. 23, no. 5, pp. 2477–2488, Sep. 2008.

[11] P. K. Steimer, J. K. Steinke, and H. E. Gruning, "A reliable, interfacefriendly medium voltage drive based on the robust igct and dtc technologies,"in *Proc. 34th IAS Annu. Meeting Ind. Appl. Conf. Record 1999IEEE*, Oct. 3–7, vol. 3, pp. 1505–1512.

[12] K.-B. Lee, J.-H. Song, I. Choy, and J.-Y. Yoo, "Torque ripple reduction in dtc of induction motor driven by three-level inverter with low switching frequency," *IEEE Trans. Power Electron.*, vol. 17, no. 2, pp. 255–264, Mar. 2002.

[13] A. Gharakhani and A. Radan, "Analytical study of affecting characteristic of voltage vectors of a three-level NPC inverter on torque and flux of DTC controlled drives," in *Proc. IEEE Int. Electr. Mach. Drives Conf. 2007*, May 3–5, vol. 1, pp. 754–759.

[14] G. Brando and R. Rizzo, "An optimized algorithm for torque oscillation reduction in dtc-induction motor drives using 3-level npc inverter," in *Proc. IEEE Int. Symp. Ind. Electron.*, May 4–7, 2004, vol. 2, pp. 1215–1220.

[15] X. del Toro Garcia, A. Arias, M. Jayne, and P. Witting, "Direct torque control of induction motors utilizing three-level voltage source inverters," *IEEE Trans. Ind. Electron.*, vol. 55, no. 2, pp. 956–958, Feb. 2008.

[16] Y. Zhang, J. Zhu,Y. Guo,W. Xu,Y.Wang, and Z. Zhao, "A sensorlessDTC strategy of induction motor fed by three-level inverter based on discrete space vector modulation," in *Proc. Australasian Univ. Power Eng. Conf. 2009*, pp. 1–6.

[17] Y. Zhang, Z. Zhao, J. Zhu, W. Xu, and D. G. Dorrell, "Speed sensorless direct torque control of 3-level inverter-fed inductionmotor drive based on optimized switching table," in *Proc. 35th Annu. Conf. IEEE Ind. Electron. 2009*, pp. 1316–1321.

[18] A. Sapin, P. K. Steimer, and J.-J. Simond, "Modeling, simulation, and test of a three-level voltage-source inverter with output lc filter and direct torque control," *IEEE Trans. Ind. Appl.*, vol. 43, no. 2, pp. 469–475, Mar./Apr. 2007.

[19] Y. Zhang, Z. Zhao, T. Lu, and L. Yuan, "Sensorless 3-level inverter-fed induction motor drive based on indirect torque control," in *Proc. IEEE 6th Int. Power Electron. Motion Control Conf. 2009*, pp. 589–593.

[20] W. S. H. Wong and D. Holliday, "Minimisation of flux droop in direct torque controlled induction motor drives," in *IEEE Proc. -Electr. Power Appl.*, Nov. 7, 2004, vol. 151, no. 6, pp. 694–703.